

## Optical properties of single coupled plasmonic nanoparticles

Cite this: *Phys. Chem. Chem. Phys.*, 2013, **15**, 4100

Lianming Tong,<sup>a</sup> Hong Wei,<sup>a</sup> Shunping Zhang,<sup>a</sup> Zhipeng Li<sup>b</sup> and Hongxing Xu<sup>\*acd</sup>

The electromagnetic (EM) coupling between metal nanoparticles (NPs) is of essential importance in nanoplasmonic systems, leading to a variety of fundamental studies and practical applications. The successive investigations in this field not only bring forward surprising optical effects in nanoplasmonics, but also allow revealing other novel chemical/physical properties in relevant systems. In this article, we will discuss the EM coupling in four types of typical plasmonic nanostructures, *i.e.*, single aggregated metal NPs, asymmetric metal NPs dimers, nano-manipulated metal NPs and supported metal NPs on a substrate, and outlook the corresponding impacts in understanding physics and extending applications.

Received 4th December 2012,  
Accepted 21st January 2013

DOI: 10.1039/c3cp44361b

[www.rsc.org/pccp](http://www.rsc.org/pccp)

### Introduction

Metal nanoparticles (NPs) possess novel optical properties due to the collective oscillation of conduction electrons, the

so-called localized surface plasmon resonance (LSPR).<sup>1</sup> Once excited by an external optical field at appropriate frequency, localized surface plasmons (LSPs) produce enormous local electromagnetic (EM) fields around metal NPs and modify the far-field emission of any emitters in the metal NPs system. These intrinsic characteristics of LSPs give rise to a variety of unique optical phenomena, leading to abundant research topics in nanoplasmonics such as surface-enhanced spectroscopy,<sup>2</sup> LSPR sensing,<sup>3</sup> plasmon-induced optical forces<sup>4</sup> and nano-lasers (SPASER).<sup>5</sup>

The optical properties of a single metal NP and coupled metal NPs have been extensively studied in both theory and experiments.<sup>6–9</sup> Two metal NPs brought into the vicinity of each

<sup>a</sup> Beijing National Laboratory for Condensed Matter Physics and Institute of Physics, Chinese Academy of Sciences, Beijing 100190, China

<sup>b</sup> Beijing Key Laboratory of Nano-Photonics and Nano-Structure (NPNS), Department of Physics, Capital Normal University, Beijing 100048, China

<sup>c</sup> Center for Nanoscience and Nanotechnology, and School of Physics and Technology, Wuhan University, Wuhan 430072, China

<sup>d</sup> Division of Solid State Physics/The Nanometer Structure Consortium, Lund University, Box 118, S-22100, Lund, Sweden. E-mail: [hxxu@iphys.ac.cn](mailto:hxxu@iphys.ac.cn)



**Lianming Tong**

Lianming Tong obtained his BS and PhD degrees from College of Chemistry and Molecular Engineering, Peking University, China, in 2002 and 2007, respectively. He did his postdoctoral research in the Department of Applied Physics, Chalmers University of Technology, Sweden, before he joined the Institute of Physics, Chinese Academy of Sciences, China, in 2011. He is currently an Associate Professor in the

Nanoscale Physics and Devices Laboratory of the institute. His research interests focus on surface-enhanced spectroscopy, near-field optical microscopy, optical manipulation, and possible applications in chemo/biosensors and devices.



**Hong Wei**

Hong Wei is currently an Associate Professor at Institute of Physics, Chinese Academy of Sciences (IOP, CAS). She received her BS degree in Physics from Shandong University, China, in July 2004, and PhD degree from IOP, CAS, in July 2009. Her research interests are focused on surface-enhanced spectroscopy, plasmonic waveguides and circuits, interactions of surface plasmons and excitons.

other's near-fields couple electromagnetically to a great extent, resulting in interesting optical properties that are unattainable by single metal NPs.<sup>6,10</sup> One of the most pronounced phenomena is the extra EM-field enhancement at the gaps that enables single molecule detection.<sup>8,11</sup> The near-field distribution sensitively depends on the incident polarization, an adjustable external parameter that can in principle switch the emission signal on and off. For more complex NP-clusters, such as NP chains and oligomers,<sup>12–14</sup> the orientation of particles plays crucial roles in engineering multiple plasmonic modes and the corresponding optical response. In the context of so-called nanoantennas, the metal NPs aggregate enhances the incident EM field, and re-scatters after modification in the near-field regime through the interplay between the LSPs of each metal NP excited by the emission of molecular dipoles. Together with the phase modulation in the far-field, the polarization and direction of the emission is dramatically tuned by LSPR,<sup>15–17</sup> leading to tunable directional emission that promises nanoscale optical devices for example, sensing and communication.



**Shunping Zhang**

*Shunping Zhang, born in 1985, currently works as a postdoctoral researcher in Professor Hongxing Xu's research group. He received his BS degree in physics in 2008 from Sun Yat-sen University, China, and got his PhD degree in 2012 from the Institute of Physics, Chinese Academy of Sciences (CAS). His current research interests include plasmonic waveguides, nano-antennas, chiral plasmonics and related applications.*



**Zhipeng Li**

*interests include the plasmonic nano-antennas, spectroscopy and theoretical simulations on nano-optics. He is a recipient of Beijing Nova of Science award.*

*Zhipeng Li was born in 1980. He received the BS degree in physics from Jilin University, China, in 2003, and the PhD degree from the Institute of Physics, Chinese Academy of Sciences (CAS), in 2008. After the research position at Nanoscale Physics and Devices Laboratory of Institute of Physics, CAS, he works at Capital Normal University (China), as a Professor in Beijing Key Laboratory of Nano-Photonics and Nano-Structure. His current research*

The EM coupling between metal NPs of different shapes is more complex due to the asymmetric geometries. The near-field distribution and polarization dependence are determined by the shapes and orientation of the nanostructures. Such characteristics are of particular interest in terms of surface-enhanced Raman scattering (SERS).<sup>18–20</sup> For example, the coupling between a metal particle and a nanohole in a metal film produces not only adequate EM enhancement for trace molecule detection, but also a “hot area” in the gap between the metal NP and the nanohole where sizable enhancement exists, rather than a regular “hot spot” between two metal NPs. This in principle does not require chemical/physical adsorption of analytes, making possible non-contact detection of molecules in a solution or gas phase.

In practice, all coupled metal NPs can be prepared using nanofabrication techniques, such as electron beam lithography (EBL), focused-ion beam (FIB) and nanosphere lithography. However, the active control of coupled metal NPs is still relatively lacking, perhaps mainly due to the demanding experimental processes. The advantages of an active control are obvious: EM coupling of *identical* metal NPs at adjustable gap distances and orientations,<sup>21–24</sup> the possibility of *in situ* investigation of optical response of a single metal NP or coupled metal NPs subject to external modifications,<sup>25,26</sup> and the precise positioning of selected single metal NPs for potential device applications.<sup>27,28</sup>

A single metal NP in a homogeneous medium is a relatively simple case, where external parameters that affect the electrons oscillation only include the dielectric constant of the sole medium and the incident EM field. Whereas on a supporting substrate, a metal NP interacts with its induced image in the substrate due to the contrast of dielectric functions between the two media, *i.e.*, symmetry breaking.<sup>29–31</sup> This is also interpreted as a special case of EM coupling, that is, the coupling between the particle and the image of itself in the substrate.

In this perspective article, we mainly focus on the EM coupling of metal NPs in different systems. The content of this article is organized as follows: In Section I, the EM coupling in



**Hongxing Xu**

*interests are in surface enhanced Raman scattering, single molecule spectroscopy, nanophotonics and plasmonics.*

*Hongxing Xu received his BS degree in Physics from Peking University, China, in July 1992, and PhD degree from Chalmers University of Technology, Sweden, in March 2002. From August 2002, he worked at the Division of Solid State Physics at Lund University, Sweden, as an Assistant Professor. In March 2005, he joined Institute of Physics, Chinese Academy of Sciences, China, where he is now a Professor. His research*

single aggregated metal NPs will be reviewed, in particular, the near-field enhancement and the emission management. Section II discusses in more detail a type of asymmetric coupling revealed by SERS, *i.e.*, the EM coupling in particle-hole pairs and the coupling between single metal NP and a metal nanowire. Along the line of coupled metal NPs in this article, Section III deals with the EM coupling between nano-manipulated metal NPs and its relevant practical applications. In Section IV, we will discuss the optical properties of supported metal NPs, with emphasis on the role the substrate may play. A summary and perspective is given at the end of this article.

## Single aggregated metal NPs

For a dimer of NPs, the excitation of the longitudinal LSP mode produces much stronger EM near-fields than the transverse mode, proven by electrodynamic simulations and experimental measurements more than one decade ago.<sup>6,10,32,33</sup> The physical picture of the near-field plot around a dimer of metal NPs shown in Fig. 1 is still the root of explanations to a series of experimental observations in the classical regime,<sup>32,34</sup> for example, redshift/blueshift of longitudinal/transverse mode<sup>35,36</sup> and increased Raman enhancement with respect to the decreased gap distance.<sup>37</sup> It is seen that the near-field is concentrated at the gap in the metal NPs dimer, and the magnitude is strongly dependent on the excitation polarization. The highest EM field is obtained with polarization parallel to the dimer axis, whereas the EM field is almost identical as that of a single metal NP if the polarization is perpendicular. The radius of Ag NPs and the gap distance shown in Fig. 1 are 45 nm and 5.5 nm, respectively. We note that such a near-field picture holds for almost all coupled dimers.

In essence, the magnitude and phase of the EM fields of a metal NP aggregate and the interplay with emission from vicinal molecules in near- and far-fields determine the optical

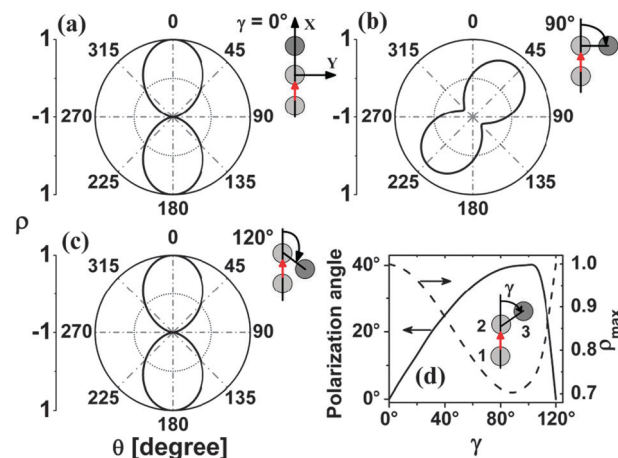


**Fig. 2** Depolarization ratio of the emission from a dipole (represented by the red arrows) at the gap between Ag particle 1 and 2 (see inset in (d)) with respect to the position of particle 3. Particle radius: 40 nm. Emission wavelength: 555 nm. Reprinted with permission from (ref. 15). Copyright (2009) American Chemical Society.

behavior of the coupled system. The Raman signal from molecules is enhanced by the local EM fields at gaps, and further, re-scattered by the metal NPs, the so-called “antenna” effect. The polarization and emission angle are both modified due to the dipole-metal NPs coupling.<sup>15–17,38</sup> Z. Li *et al.* studied the polarization of the emission of a dipole located at the gap of a dimer and at one of the gaps of a trimer of Ag NPs.<sup>15</sup> In Fig. 2, the red arrows represent the orientation of the dipole, and the geometry of the metal NPs is shown in the inset of Fig. 2d. Apparently, the depolarization ratio strongly depends on the position of the third particle. For the axial symmetric configuration in Fig. 2a, the emitted light from the dipole is linearly polarized along the axis, identical to the dimer case. However, the polarization was rotated by 40° clockwise (Fig. 2b) when the third particle is positioned to the right of the middle one due to

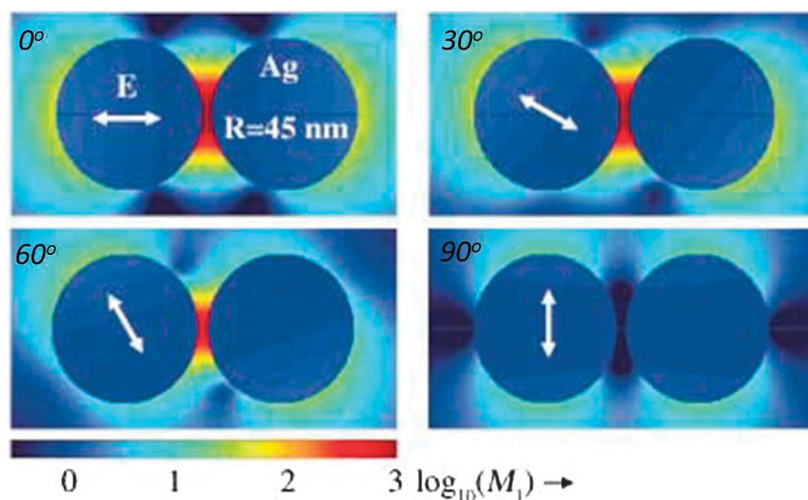


**Fig. 1** Near-field plots of a dimer of Ag NPs (diameter 90 nm, gap distance 5.5 nm) at different polarization angles given in the top-left of each panel. Excitation wavelength: 514.5 nm. Adapted with permission from (ref. 32). Copyright © 2003 WILEY-VCH Verlag GmbH & Co. KGaA, Weinheim.

the asymmetric coupling. If the three particles are oriented in an equilateral triangle, the polarization is further rotated back because particle 3 couples to particles 1 and 2 symmetrically in this case, as shown in Fig. 2c. Fig. 2d shows the polarization angles with respect to the position of the third particle moved around the second one.

The plasmon coupling between the third particle and the other two affects the polarization and ellipticity of the far-field emission. The complex coupling in the trimer nanoantenna system results in multiple plasmon resonances. Around each resonance peak, the polarization angle differs for each emission wavelength. In Fig. 3a, the change of polarization angles around the  $\sim 520$  nm resonance is shown. As the resonant peak positions can be tuned by varying the refractivity of the circumstance  $n_s$ , it consequently leads to the alternating of the polarization angle for one specific wavelength. An example of the dipole emission at 555 nm is shown in Fig. 3b. It is seen that the polarization of the emission changes sharply with variation of  $n_s$ . A  $90^\circ$  rotation was found by changing the refractive index from 1.0 to 1.5. The sensitive transition of the emission polarization in the trimer nanoantenna system to  $n_s$  has potential applications aiming at controlling the polarization status of the dipole emission.

Along with the polarization tuning, the directional emission from a dimer of metal NPs has also been reported.<sup>17,38</sup> Fourier imaging of SERS shows that, enhanced by a dimer of Au NPs, the Raman emission is preferentially directed to angles that are orthogonal to the dimer axis, whereas in a symmetric trimer case, the emission is also symmetric.<sup>38</sup> More interestingly, the Rayleigh scattered light by a dimer of bimetallic NP, *i.e.*, gold

and silver, is split into different directions with respect to wavelength: “blue” light toward the Ag side and “red” light toward the Au side due to the constructive/destructive interference of the scattered light of different wavelengths to different directions.<sup>17</sup> This in principle realizes a nanoscale color router that simply relies on asymmetric material composition.

The nano-antennas based on NP-aggregates would find promising applications in nanoplasmonics and nanooptics, for example, to improve the efficiency of optical sensors that combines with the new emerging graphene,<sup>39</sup> to make possible the control of the emission polarization and direction of SPASER,<sup>40</sup> and to tune actively ultra-fast optical switches by other functional materials.<sup>41,42</sup> However, one of the bottlenecks that obstruct its future development lies in the fine control of the geometry of the nano-aggregate. The combination of chemical synthesis and nanofabrication such as EBL and FIB<sup>43</sup> could be one of the potential solutions.

## Coupling of asymmetric metal NPs for SERS

The nanogaps in metal NPs aggregates provide hot-spots for large Raman enhancement. Nanoholes in a metal film, a type of “negative” NPs, also exhibit interesting optical properties. The EM coupling between a “positive” (nanoparticle) and a “negative” (nanohole) metal NP is expected to be distinct from that between two “positive” ones, simply due to the geometric asymmetry. Nanohole arrays in a metal film have been employed for SERS substrates.<sup>44,45</sup> For single isolated nanohole, due to the relatively weaker confinement of the EM field, it normally cannot produce sufficient Raman enhancement for the probe molecules. However, if a metal NP is put into a nanohole, EM coupling occurs between the hole and the particle, making significant SERS enhancement possible. In experiments, nanoholes in a gold film can be fabricated using self-assembly colloidal lithography.<sup>19</sup> With selective chemical modifications of the gold surface and the glass substrate in the holes by different chemicals (Fig. 4a), gold NPs can be assembled into the holes, thus forming a hole-particle pair (Fig. 4b). The Raman signals of malachite green isothiocyanate (MGITC) molecules were measured on different hole-particle pairs. For a single nanohole in gold film, very weak Raman signal was observed, mainly owing to the excitation of LSPR in the rough gold surface. Instead, for a hole-particle pair, the Raman signal was about 100 times stronger (Fig. 4c). Since the gold NP is smaller than the nanohole and the NP was located off the center of the hole, a “hot area” is formed in the small nanogap, where sizable EM enhancement exists. The electric field distribution in the hole-particle pair was calculated using three-dimensional finite difference time domain (FDTD) method. As can be seen from the inset in Fig. 4c, the local electric field in the junction between the nanohole and the NP is largely enhanced. The smaller distance between the hole wall and the particle results in larger electric field enhancement. Also note that such a “hot area” in the hole-particle pair is much larger in volume than the “hot spots” in metal NPs aggregates, which makes the hole-particle pair system suitable

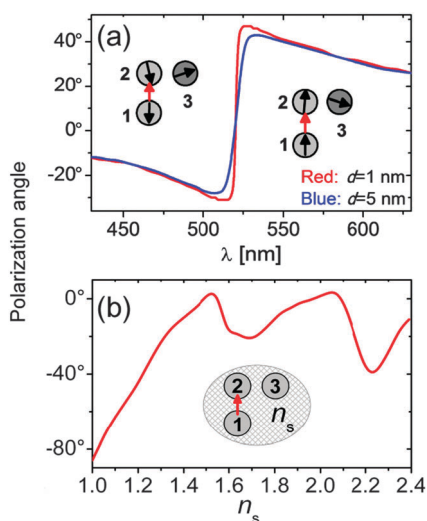


**Fig. 3** (a) Polarization angle as a function of the wavelength of the dipole emission for the right-angle configuration of a silver trimer antenna with identical NPs ( $R = 40$  nm). The separation between the 1st and 2nd NPs is either  $d = 1$  nm (red) or  $d = 5$  nm (blue). The separation between the 2nd and 3rd NPs is kept constant at 1 nm. Black arrows in insets: representations of the dipolar polarization excited in each NP. (b) Polarization angle of a dipole located between particle 1 and 2 vs. refractive index of the surrounding media ( $n_s$ ). The radii of the particles are 40 nm for particle 1 and 2, and 80 nm for particle 3. The dipole emits at 555 nm. Reprinted with permission from (ref. 15). Copyright (2009) American Chemical Society.

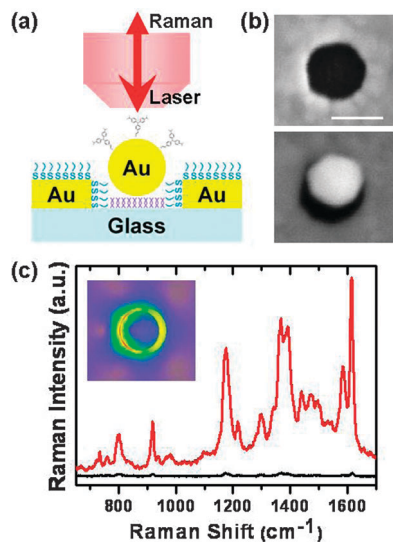


**Fig. 4** (a) Sketches for the sample and the optical measurement. (b) The scanning electron microscopy (SEM) images of single nanohole (top) and single hole-particle pair (bottom). The scale bar is 100 nm. (c) The SERS spectra measured on a single nanohole (black) and on a single hole-particle pair (red). The inset shows the electric field distribution calculated using FDTD method. Adapted with permission from (ref. 19). Copyright © 2003 WILEY-VCH Verlag GmbH & Co. KGaA, Weinheim.

for applications in detection of molecules without physical contact with metals and the substrate. By optimizing the size match of the nanoparticle and the nanohole, larger hot areas can be obtained.

The coupling between a metal NP and a metal nanowire can also generate strongly enhanced EM field. The experimental investigations show that the nanowire-NP coupled structures (Fig. 5a) are quite efficient for Raman enhancement.<sup>20</sup> It is found that the enhancement is strongly dependent on the polarization of the excitation light. When the laser polarization is perpendicular to the nanowire, the SERS enhancement is maximal, whereas the Raman signal is the weakest when the laser is polarized parallel to the nanowire. The calculated electric field distributions under parallel and perpendicular polarizations are shown in Fig. 5b. Apparently, for perpendicular polarization, hot spot appears at the wire-particle junction. Detailed measurements on polarization dependence show that the SERS intensity has a  $\cos^2\theta$  dependence on the laser polarization, where  $\theta$  is the angle between the polarization direction and the axis perpendicular to the nanowire. Although the Raman enhancement factor is proportional to the fourth power of the electric field enhancement, only the excitation field enhancement is dependent on the polarization, which has a  $\cos^2\theta$  dependence. For the emission enhancement, it is determined by the antenna structure and not dependent on the excitation polarization. Therefore, the total Raman enhancement shows the  $\cos^2\theta$  dependence, instead of  $\cos^4\theta$  dependence.

Different from NPs, metal nanowires can function as waveguides to support the propagation of surface plasmon polaritons (SPPs).<sup>46</sup> If a laser is incident on the terminal of the nanowire, SPPs on the nanowire are excited and propagate along the nanowire. The properties of SPPs on metal nanowires

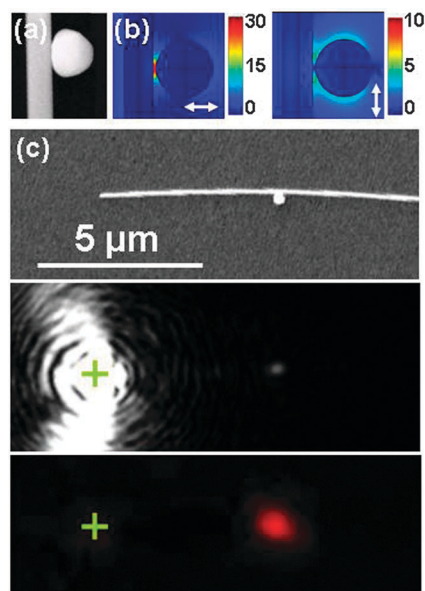


**Fig. 5** (a) SEM image of a metal nanowire-NP structure. (b) Calculated electric field distribution in a nanowire-NP structure for polarization perpendicular (left) and parallel (right) to the nanowire. The radii of the NP and the nanowire are 50 nm and 25 nm, respectively. The gap distance between the nanowire and the NP is 5 nm. (c) The remote-excitation SERS in a nanowire-NP structure. Adapted with permission from (ref. 18 and 20). Copyright (2009) American Chemical Society (ref. 18) and Copyright (2008) American Chemical Society (ref. 20).

have been intensively investigated recently.<sup>47–61</sup> By using propagating surface plasmons, the hot spot between the nanowire and the NP can be excited without shining light directly onto the nanowire-NP junction.<sup>18,62</sup> For the silver nanowire-NP structure shown in Fig. 5c, laser light of 633 nm was focused on the left end of the nanowire. The bright spot at the right 6 μm away from the laser spot (middle panel in Fig. 5c) is a result of the guiding surface plasmons along the nanowire, which are partly scattered out at the junction. The Raman image obtained by using the intensity of a specific Raman peak for the probe molecule shows that the strong Raman signal is only obtained at the wire-particle junction (bottom panel in Fig. 5c). That is to say, the SERS signal at the hot spot is remotely excited. The remote excitation configuration has prominent advantages compared with direct excitation. First, the junction between the nanowire and the NP has a very small area of nanometer scale, which makes it a nanoscale light source. Second, the nanoscale illumination area makes the Raman detection almost free from the background noise. Third, the nanoscale excitation avoids strong light illumination over large area which may cause damages to the samples. We experimentally show that the remote-excitation SERS has single-molecule sensitivity. Besides, multi-site remote-excitation can be realized simultaneously in the structures with multiple hot spots.

## Coupling of nano-manipulated metal NPs

A demanding challenge in studying the optical properties of single and aggregated metal NPs and using it in device applications is the

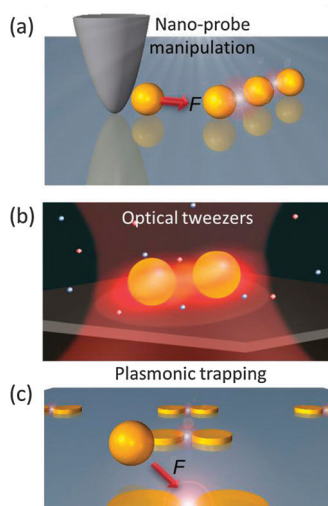


**Fig. 6** Schematic drawings of different manipulation techniques. (a) Nano-probe manipulation. (b) Optical tweezers. (c) Plasmonic trapping.

selective location of a single particle of interest in a solution and the accurate positioning of particles on a substrate. A variety of manipulation techniques have thus been endeavored to along this line. Typical examples include nano-probe manipulation, in particular, scanning probe microscopy (SPM), that deals with single particles on a supporting substrate,<sup>21,27,28</sup> optical tweezers that can trap free-floating particles in an aqueous solution<sup>63–65</sup> and plasmonic trapping that uses pre-defined plasmonic nanostructures on a substrate.<sup>4,66</sup> Fig. 6 schemes such manipulation techniques. Here it is also worth noting that electrical force manipulation such as dielectrophoresis using an external alternating electric field can simultaneously move and orientate multiple NPs in a solution.<sup>67</sup>

Nanoprobe manipulation of NPs on a substrate has been previously demonstrated, for example, to deposit single gold NP on a conductive substrate using scanning tunneling microscope (STM) for electrical study<sup>27</sup> and to selectively transfer a single gold NP from one substrate to another using a chemically modified atomic force microscopy (AFM) tip.<sup>28</sup> Olk *et al.* studied the EM coupling between two metal NPs – one attached to the apex of a tapered fiber tip and another fixed on a glass substrate mounted on a piezoelectric translation stage.<sup>21</sup> They found clear near-field coupling at short interparticle distances ( $d < 200$  nm) for both parallel and perpendicular excitation polarization (Fig. 7a). However, a strong modulation (periodicity  $\sim 350$  nm) of the resonance peak widths and peak positions was observed at larger separations if the polarization is perpendicular to the axial direction of the two particles, which was due to the interference of the corresponding scattering by the two individual particles. AFM-manipulated aggregates of gold NPs for SERS has also been reported.<sup>22,68</sup> Despite the fact that the interparticle distances were not identical in all the structures, a much more rapid increase of the enhancement factor was observed (Fig. 7b) with increased number of particles ( $\sim 60$  nm in diameter) aligned in a row under 633 nm laser excitation of parallel polarization than perpendicular, attributed

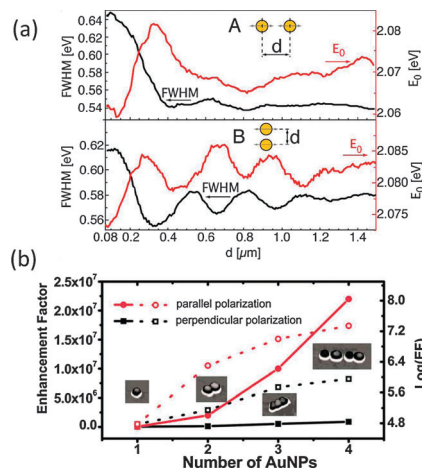


**Fig. 7** (a) Optical response of two gold NPs, one fixed on the substrate and the other manipulated by a tapered optical fiber. Full width at half maximum (FWHM) (left y-axis) and peak position (right y-axis) in energy scale (eV) of the two gold NPs as a function of interparticle distance under parallel (upper panel) and perpendicular (lower panel) excitation polarizations. (b) SERS enhancement factor of AFM-manipulated gold NPs ( $\sim 60$  nm) vs. number of particles aligned in a row under 633 nm excitation with parallel polarization. Adapted with permission from (ref. 21 and 22). Copyright (2008) American Chemical Society (ref. 21) and Copyright (2008) American Institute of Physics (ref. 22).

to the much more effective near-field coupling in the former case.

Optical tweezers are powerful manipulation tools that can capture and release NPs in a solution. Metallic NPs, despite the much larger absorption and scattering cross sections than dielectrics, have been proven stable for 3-dimensional optical trapping using a single focused laser beam.<sup>63,65</sup> The work by S. M. Block *et al.* in 1994 was considered to be one of the pioneering demonstrations.<sup>65</sup> Thereafter, a series of optical trapping techniques have been used to manipulate colloidal metal NPs and study their optical response *in situ*, including single focused Gaussian beam,<sup>63</sup> single focused doughnut-shaped beam (Larguerre–Gaussian),<sup>69</sup> counter-propagating beams<sup>70</sup> and plasmonic tweezers.<sup>66,71</sup> Many interesting topics have consequently emerged in this aspect, such as the force interactions between trapped NPs,<sup>26</sup> the *in situ* optical response of a single trapped particle subjected to chemical reaction,<sup>25</sup> and the optical heating effect of single metal NPs.<sup>72</sup> Fig. 8a shows the dark-field (DF) scattering spectra and imaging of a dimer of trapped gold NPs ( $\sim 80$  nm in diameter) with illuminating electric field parallel and perpendicular to the trapping laser polarization, or in other words, the dimer axis,<sup>26</sup> respectively, in an aqueous solution with different salt (NaCl) concentrations. It is seen that the longitudinal LSPR peak redshifts with increased ionic strength due to the decreased surface screening, and thus shorter interparticle distances and stronger EM coupling. The forces involved are rather complex—optical forces from the laser beam and due to the excitation of LSPR in the particles,<sup>73–75</sup> Coulomb force that relies on the number of surface charges, and van der Waals force that depends on an intrinsic physical parameter, *i.e.*, Hamaker constant—all sensitively determined by the interparticle distance. Given suitable

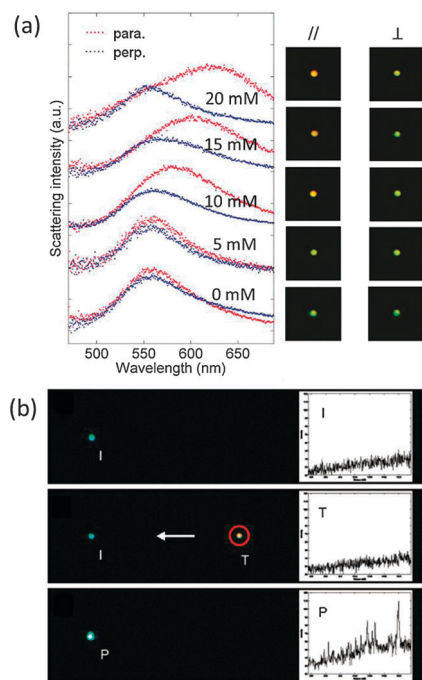


**Fig. 8** (a) Dark-field (DF) scattering spectra and images of a dimer of  $\sim 80$  nm gold NPs in an optical trap with different NaCl concentrations under parallel and perpendicular polarizations of white light with respect to the dimer axis. (b) SERS signal was observed when two Ag NPs were brought close to each other using optical tweezers. Top, middle and bottom panels represent DF images and SERS spectra from single immobilized, single trapped and dimerized Ag NPs. Reprinted with permission from (ref. 26 and 76). Copyright (2011) American Chemical Society (ref. 26) and Copyright (2006) American Chemical Society (ref. 76).

assumptions of the Hamaker constant and surface charges, and combining the calculated optical potentials using Mie theory, the interparticle distances could be reasonably deduced.<sup>26</sup>

The possibility of multi-particle trapping enables interesting applications in SERS sensing.<sup>76–78</sup> Using a 2-dimensional trap, F. Svedberg *et al.* showed dramatic SERS enhancement by moving a trapped Ag NP close to a fixed one on a glass slide, whereas no SERS signal was observed from either of the single particles (Fig. 8b). Brought close to each other, a sharp optical potential well appears due to the EM coupling under the excitation of the trapping laser.<sup>79</sup> This results in an attractive optical force that would bring them even closer, creating a so-called “hot spot” for SERS.<sup>73,76</sup> It is worth noting that, with more surface charges, *i.e.*, a stronger Coulomb repulsive force, such a dimerization process is reversible – if the trapping laser is blocked, one sees two particles escape freely into the colloidal solution.<sup>26</sup>

Such nanomanipulation techniques enable the optical study of *identical* metal NPs, which excludes the geometry inhomogeneity effect to a great extent. However, certain disadvantages still limit more detailed optical investigation. For example, the contamination of nano-probe manipulated NPs by the probe itself complicates the optical response of NPs, especially in SERS. For optically trapped NPs, thermal effect is one of major problems that cause destabilization. Such limitations should be fully considered in future studies.

## Supported metal NPs

In most realistic studies, the NPs are usually deposited on a substrate, either dielectric or metallic. The presence of the nearby dielectric substrate can break the symmetry of the system, which mediates the coupling between the primitive localized plasmon modes in the metallic NPs<sup>30,31</sup> or primitive SPPs in extended metallic structures.<sup>29</sup> The substrate effects can be interpreted using an image charges picture, which can be modeled by extending the standard Mie theory.<sup>80–82</sup> The strengths of the images are screened by a factor of  $(\epsilon_s - 1)/(\epsilon_s + 1)$ , where  $\epsilon_s$  is dielectric constant of substrate.<sup>83</sup> For higher permittivity substrate, the coupling to the images becomes stronger so that the frequently used effective permittivity treatment for the substrate effect becomes too simple to predict all the effects, such as energies shift, mode degeneracies and field distributions, *etc.* In modeling the excitation of SPPs in NPs-over-substrate system by, for example, a plane wave, both the incident and reflected light by the substrate should be included as input. This can be taken into account by modifying the incident formula in the Mie theory or using the analytical solution of the air–dielectric interface (Fresnel formula) as background field in the finite element method.<sup>84</sup>

The interaction with dielectric substrate is stronger for a NP with a planar contacting surface to the substrate, for example, a silver nanocube.<sup>84,85</sup> When a cube is moved from far away to being contacted with a substrate, the dipolar mode (D mode) is greatly redshifted. On the contrary, the quadrupolar mode (Q mode) undergoes a small energy shift but is getting stronger in the optical spectrum. These behaviors are the consequences of substrate-mediated coupling, as schematically shown in Fig. 9a. The coupling mixes the primitive plasmon modes (denoted  $D^0$  and  $Q^0$ ) such that the otherwise dark mode ( $Q^0$ ) becomes bright in the optical spectrum due to the dipole moment obtained from the coupling. Interestingly, when the interaction *via* substrate is not very strong so that the D mode and Q mode are not far apart, the interference between these two modes can lead to a Fano lineshape in the scattering spectrum.<sup>84</sup> Such substrate-induced Fano resonances can also be observed in a supported gold nanorod, where the interaction occurs between a broad octupolar and a narrow quadrupolar plasmon mode.<sup>86</sup>

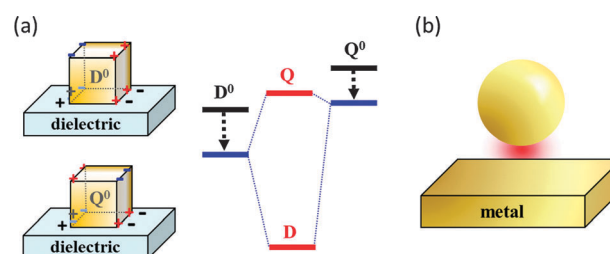


**Fig. 9** (a) Dielectric substrate mediated plasmon coupling of the dipolar (D) and quadrupolar (Q) mode in a metal nanocube. Reprinted with permission from (ref. 84) Copyright (2011) American Chemical Society. (b) Strong coupling of metal NP near a metal surface leads to hot spot in the particle–film junction.

The coupling of a NP with a nearby metallic substrate, as shown in Fig. 9b, is similar to the coupling between two adjacent NPs, with giant EM field enhancement in the gap region. The shift of plasmon energies in the NP can be predicted by a plasmon hybridization model in the non-retardation region.<sup>33</sup> Due to the extended characteristic of the metal surface, these interactions occur between the LSPs in the NP and the SPPs in the metal substrate in analogue of the Anderson model.<sup>87</sup> Interesting phenomenon such as virtual states can be realized in such system by adjusting the thickness of the metal film. Beside the theoretical aspect, such NP over metal mirror (NPOM) is attractive also in the point of view of fabrication.<sup>88–93</sup> By using molecule linker,<sup>88</sup> thin dielectric shell<sup>89</sup> or atomic-layer-deposited spacer layer,<sup>91</sup> it is achievable in practice to precisely control the NP-film separation and investigate the NPOM system in great details. Benefitting from such high precision fabrication, it has been made possible to test the nonlocal effect in a nearly contact metallic junction by utilizing the NPOM system.<sup>93</sup> On the other hand, this system is naturally a highly reliable, large-area and cost-efficient SERS substrate.

In the NP dimer case, maximum field enhancement can be achieved when the excitation light is incident normal to the dimer axis with the electric field polarized parallel to the dimer axis.<sup>94</sup> However, the reflected light from the metal surface can make things different in the NPOM. As the incident angle (angle between the  $k$ -vector of the incident light and the substrate normal) increases, the superposition of the incident and reflected light reduces the normal component of the excitation field.<sup>95</sup> As a result, there exists an optimized incident angle at which the local field enhancement at the NP-film junction reaches its maximum.<sup>91</sup>

## Summary and perspective

In this article, we reviewed the EM coupling of aggregated metal NPs, including single aggregated metal NPs, metal NPs of different geometry, nano-manipulated metal NPs and the coupling between a single metal NP and its induced image in a supporting substrate. Many of the optical properties of such coupled metal NPs have been observed and well-interpreted using classical electrodynamic simulations. Recently, novel effects originated from the coupling between metal NPs have also been shown, for example, the Fano resonance in heterodimers and oligomers<sup>9,96,97</sup> and quantum plasmonic effects in sub-nanometer gaps.<sup>98–100</sup> Besides the so-far reported fundamental characteristics and vast applications, it can be foreseen that, along with the rapid progress in plasmonics, new optical phenomena could be predicted and observed due to the strong EM coupling of metal NPs, which is of essential importance in nanoplasmonic systems.

## Acknowledgements

This work was supported by MOST Grants (No. 2009CB930700), NSFC Grants (Nos. 11004237, 11134013, 11227407, 11274004) and “Knowledge Innovation Project” (KJCX2-EW-W04) of CAS.

## References

- 1 E. Hutter and J. H. Fendler, *Adv. Mater.*, 2004, **16**, 1685–1706.
- 2 M. Moskovits, *Rev. Mod. Phys.*, 1985, **57**, 783–826.
- 3 K. A. Willets and R. P. Van Duyne, *Annu. Rev. Phys. Chem.*, 2007, **58**, 267–297.
- 4 M. L. Juan, M. Righini and R. Quidant, *Nat. Photonics*, 2011, **5**, 349–356.
- 5 M. I. Stockman, *Nat. Photonics*, 2008, **2**, 327–329.
- 6 E. Hao and G. C. Schatz, *J. Chem. Phys.*, 2004, **120**, 357–366.
- 7 M. M. Miller and A. A. Lazarides, *J. Phys. Chem. B*, 2005, **109**, 21556–21565.
- 8 H. X. Xu, E. J. Bjerneld, M. Käll and L. Borjesson, *Phys. Rev. Lett.*, 1999, **83**, 4357–4360.
- 9 N. J. Halas, S. Lal, W. S. Chang, S. Link and P. Nordlander, *Chem. Rev.*, 2011, **111**, 3913–3961.
- 10 J. Aizpurua, G. W. Bryant, L. J. Richter, F. J. G. de Abajo, B. K. Kelley and T. Mallouk, *Phys. Rev. B: Condens. Matter Mater. Phys.*, 2005, **71**, 235420.
- 11 S. M. Nie and S. R. Emery, *Science*, 1997, **275**, 1102–1106.
- 12 S. J. Barrow, A. M. Funston, D. E. Gómez, T. J. Davis and P. Mulvaney, *Nano Lett.*, 2011, **11**, 4180–4187.
- 13 L. S. Slaughter, B. A. Willingham, W. S. Chang, M. H. Chester, N. Ogden and S. Link, *Nano Lett.*, 2012, **12**, 3967–3972.
- 14 J. A. Fan, K. Bao, L. Sun, J. M. Bao, V. N. Manoharan, P. Nordlander and F. Capasso, *Nano Lett.*, 2012, **12**, 5318–5324.
- 15 Z. P. Li, T. Shegai, G. Haran and H. X. Xu, *ACS Nano*, 2009, **3**, 637–642.
- 16 T. Shegai, Z. P. Li, T. Dadosh, Z. Y. Zhang, H. X. Xu and G. Haran, *Proc. Natl. Acad. Sci. U. S. A.*, 2008, **105**, 16448–16453.
- 17 T. Shegai, S. Chen, V. D. Miljković, G. Zengin, P. Johansson and M. Käll, *Nat. Commun.*, 2011, **2**, 481.
- 18 Y. R. Fang, H. Wei, F. Hao, P. Nordlander and H. X. Xu, *Nano Lett.*, 2009, **9**, 2049–2053.
- 19 H. Wei, U. Håkanson, Z. L. Yang, F. Hook and H. X. Xu, *Small*, 2008, **4**, 1296–1300.
- 20 H. Wei, F. Hao, Y. Z. Huang, W. Z. Wang, P. Nordlander and H. X. Xu, *Nano Lett.*, 2008, **8**, 2497–2502.
- 21 P. Olk, J. Renger, M. T. Wenzel and L. M. Eng, *Nano Lett.*, 2008, **8**, 1174–1178.
- 22 L. Tong, T. Zhu and Z. Liu, *Appl. Phys. Lett.*, 2008, **92**, 023109.
- 23 F. M. Huang and J. J. Baumberg, *Nano Lett.*, 2010, **10**, 1787–1792.
- 24 K. D. Alexander, K. Skinner, S. P. Zhang, H. Wei and R. Lopez, *Nano Lett.*, 2010, **10**, 4488–4493.
- 25 W. H. Ni, H. J. Ba, A. A. Lutich, F. Jäckel and J. Feldmann, *Nano Lett.*, 2012, **12**, 4647–4650.
- 26 L. Tong, V. D. Miljković, P. Johansson and M. Käll, *Nano Lett.*, 2011, **11**, 4505–4508.
- 27 G. H. Yang, L. Tan, Y. Y. Yang, S. W. Chen and G. Y. Liu, *Surf. Sci.*, 2005, **589**, 129–138.

- 28 Y. Tanaka and K. Sasaki, *Appl. Phys. Lett.*, 2010, **96**, 053117.
- 29 S. P. Zhang and H. X. Xu, *ACS Nano*, 2012, **6**, 8128–8135.
- 30 Y. P. Wu and P. Nordlander, *J. Phys. Chem. C*, 2010, **114**, 7302–7307.
- 31 M. W. Knight, Y. P. Wu, J. B. Lassiter, P. Nordlander and N. J. Halas, *Nano Lett.*, 2009, **9**, 2188–2192.
- 32 H. X. Xu and M. Käll, *ChemPhysChem*, 2003, **4**, 1001–1005.
- 33 P. Nordlander and E. Prodan, *Nano Lett.*, 2004, **4**, 2209–2213.
- 34 S. K. Ghosh and T. Pal, *Chem. Rev.*, 2007, **107**, 4797–4862.
- 35 L. Gunnarsson, T. Rindzevicius, J. Prikulis, B. Kasemo, M. Käll, S. L. Zou and G. C. Schatz, *J. Phys. Chem. B*, 2005, **109**, 1079–1087.
- 36 P. K. Jain, W. Y. Huang and M. A. El-Sayed, *Nano Lett.*, 2007, **7**, 2080–2088.
- 37 J. Jiang, K. Bosnick, M. Maillard and L. Brus, *J. Phys. Chem. B*, 2003, **107**, 9964–9972.
- 38 T. Shegai, B. Brian, V. D. Miljković and M. Käll, *ACS Nano*, 2011, **5**, 2036–2041.
- 39 W. G. Xu, X. Ling, J. Q. Xiao, M. S. Dresselhaus, J. Kong, H. X. Xu, Z. F. Liu and J. Zhang, *Proc. Natl. Acad. Sci. U. S. A.*, 2012, **109**, 9281–9286.
- 40 M. A. Noginov, G. Zhu, A. M. Belgrave, R. Bakker, V. M. Shalaev, E. E. Narimanov, S. Stout, E. Herz, T. Suteewong and U. Wiesner, *Nature*, 2009, **460**, 1110–1113.
- 41 M. Abb, P. Albella, J. Aizpurua and O. L. Muskens, *Nano Lett.*, 2011, **11**, 2457–2463.
- 42 N. Large, M. Abb, J. Aizpurua and O. L. Muskens, *Nano Lett.*, 2010, **10**, 1741–1746.
- 43 J. S. Huang, V. Callegari, P. Geisler, C. Bruning, J. Kern, J. C. Prangma, X. F. Wu, T. Feichtner, J. Ziegler, P. Weinmann, M. Kamp, A. Forchel, P. Biagioni, U. Sennhauser and B. Hecht, *Nat. Commun.*, 2010, **1**, 150.
- 44 A. G. Brolo, E. Arctander, R. Gordon, B. Leathem and K. L. Kavanagh, *Nano Lett.*, 2004, **4**, 2015–2018.
- 45 Q. M. Yu, P. Guan, D. Qin, G. Golden and P. M. Wallace, *Nano Lett.*, 2008, **8**, 1923–1928.
- 46 H. Wei and H. X. Xu, *Nanophotonics*, 2012, **1**, 155–169.
- 47 H. Ditlbacher, A. Hohenau, D. Wagner, U. Kreibitz, M. Rogers, F. Hofer, F. R. Aussenegg and J. R. Krenn, *Phys. Rev. Lett.*, 2005, **95**, 257403.
- 48 A. W. Sanders, D. A. Routenberg, B. J. Wiley, Y. N. Xia, E. R. Dufresne and M. A. Reed, *Nano Lett.*, 2006, **6**, 1822–1826.
- 49 M. Allione, V. V. Temnov, Y. Fedutik, U. Woggon and M. V. Artemyev, *Nano Lett.*, 2008, **8**, 31–35.
- 50 Z. P. Li, F. Hao, Y. Z. Huang, Y. R. Fang, P. Nordlander and H. X. Xu, *Nano Lett.*, 2009, **9**, 4383–4386.
- 51 H. Wei, D. Ratchford, X. Q. Li, H. X. Xu and C. K. Shih, *Nano Lett.*, 2009, **9**, 4168–4171.
- 52 Z. P. Li, K. Bao, Y. R. Fang, Z. Q. Guan, N. J. Halas, P. Nordlander and H. X. Xu, *Phys. Rev. B: Condens. Matter Mater. Phys.*, 2010, **82**, 241402.
- 53 Y. R. Fang, Z. P. Li, Y. Z. Huang, S. P. Zhang, P. Nordlander, N. J. Halas and H. X. Xu, *Nano Lett.*, 2010, **10**, 1950–1954.
- 54 Z. P. Li, K. Bao, Y. R. Fang, Y. Z. Huang, P. Nordlander and H. X. Xu, *Nano Lett.*, 2010, **10**, 1831–1835.
- 55 H. Wei, Z. P. Li, X. R. Tian, Z. X. Wang, F. Z. Cong, N. Liu, S. P. Zhang, P. Nordlander, N. J. Halas and H. X. Xu, *Nano Lett.*, 2011, **11**, 471–475.
- 56 Z. Y. Fang, L. R. Fan, C. F. Lin, D. Zhang, A. J. Meixner and X. Zhu, *Nano Lett.*, 2011, **11**, 1676–1680.
- 57 S. P. Zhang, H. Wei, K. Bao, U. Håkanson, N. J. Halas, P. Nordlander and H. X. Xu, *Phys. Rev. Lett.*, 2011, **107**, 096801.
- 58 H. Wei, Z. X. Wang, X. R. Tian, M. Käll and H. X. Xu, *Nat. Commun.*, 2011, **2**, 387.
- 59 T. Shegai, V. D. Miljković, K. Bao, H. X. Xu, P. Nordlander, P. Johansson and M. Käll, *Nano Lett.*, 2011, **11**, 706–711.
- 60 W. H. Wang, Q. Yang, F. R. Fan, H. X. Xu and Z. L. Wang, *Nano Lett.*, 2011, **11**, 1603–1608.
- 61 C. Rewitz, T. Keitzl, P. Tuchscherer, J. Huang, P. Geisler, G. Razinskas, B. Hecht and T. Brixner, *Nano Lett.*, 2012, **12**, 45–49.
- 62 J. A. Hutchison, S. P. Centeno, H. Odaka, H. Fukumura, J. Hofkens and H. Uji-i, *Nano Lett.*, 2009, **9**, 995–1001.
- 63 P. M. Hansen, V. K. Bhatia, N. Harrit and L. Oddershede, *Nano Lett.*, 2005, **5**, 1937–1942.
- 64 J. Prikulis, F. Svedberg, M. Käll, J. Enger, K. Ramser, M. Goksor and D. Hanstorp, *Nano Lett.*, 2004, **4**, 115–118.
- 65 K. Svoboda and S. M. Block, *Opt. Lett.*, 1994, **19**, 930–932.
- 66 A. N. Grigorenko, N. W. Roberts, M. R. Dickinson and Y. Zhang, *Nat. Photonics*, 2008, **2**, 365–370.
- 67 A. Jamshidi, P. J. Pauzauskie, P. J. Schuck, A. T. Ohta, P. Y. Chiou, J. Chou, P. D. Yang and M. C. Wu, *Nat. Photonics*, 2008, **2**, 85–89.
- 68 L. M. Tong, T. Zhu and Z. F. Liu, *Chem. Soc. Rev.*, 2011, **40**, 1296–1304.
- 69 M. Dienerowitz, M. Mazilu, P. J. Reece, T. F. Krauss and K. Dholakia, *Opt. Express*, 2008, **16**, 4991–4999.
- 70 M. Ploschner, T. Cizmar, M. Mazilu, A. Di Falco and K. Dholakia, *Nano Lett.*, 2012, **12**, 1923–1927.
- 71 M. Righini, A. S. Zelenina, C. Girard and R. Quidant, *Nat. Phys.*, 2007, **3**, 477–480.
- 72 A. Kyrsting, P. M. Bendix, D. G. Stamou and L. B. Oddershede, *Nano Lett.*, 2010, **11**, 888–892.
- 73 H. X. Xu and M. Käll, *Phys. Rev. Lett.*, 2002, **89**, 246802.
- 74 R. A. Nome, M. J. Guffey, N. F. Scherer and S. K. Gray, *J. Phys. Chem. A*, 2009, **113**, 4408–4415.
- 75 A. J. Hallock, P. L. Redmond and L. E. Brus, *Proc. Natl. Acad. Sci. U. S. A.*, 2005, **102**, 1280–1284.
- 76 F. Svedberg, Z. P. Li, H. X. Xu and M. Käll, *Nano Lett.*, 2006, **6**, 2639–2641.
- 77 L. M. Tong, M. Righini, M. U. Gonzalez, R. Quidant and M. Käll, *Lab Chip*, 2009, **9**, 193–195.
- 78 Y. Tanaka, H. Yoshikawa, T. Itoh and M. Ishikawa, *J. Phys. Chem. C*, 2009, **113**, 11856–11860.
- 79 Z. P. Li, M. Käll and H. Xu, *Phys. Rev. B: Condens. Matter Mater. Phys.*, 2008, **77**, 085412.
- 80 G. Videen, *J. Opt. Soc. Am. A*, 1991, **8**, 483–489.
- 81 G. Videen, *J. Opt. Soc. Am. A*, 1992, **9**, 844–845.

- 82 H. X. Xu and M. Käll, *Sens. Actuators, B*, 2002, **87**, 244–249.
- 83 K. C. Vernon, A. M. Funston, C. Novo, D. E. Gómez, P. Mulvaney and T. J. Davis, *Nano Lett.*, 2010, **10**, 2080–2086.
- 84 S. P. Zhang, K. Bao, N. J. Halas, H. X. Xu and P. Nordlander, *Nano Lett.*, 2011, **11**, 1657–1663.
- 85 L. J. Sherry, S. H. Chang, G. C. Schatz, R. P. Van Duyne, B. J. Wiley and Y. N. Xia, *Nano Lett.*, 2005, **5**, 2034–2038.
- 86 H. J. Chen, L. Shao, T. Ming, K. C. Woo, Y. C. Man, J. F. Wang and H. Q. Lin, *ACS Nano*, 2011, **5**, 6754–6763.
- 87 F. Le, N. Z. Lwin, J. M. Steele, M. Käll, N. J. Halas and P. Nordlander, *Nano Lett.*, 2005, **5**, 2009–2013.
- 88 J. J. Mock, R. T. Hill, A. Degiron, S. Zauscher, A. Chilkoti and D. R. Smith, *Nano Lett.*, 2008, **8**, 2245–2252.
- 89 J. F. Li, Y. F. Huang, Y. Ding, Z. L. Yang, S. B. Li, X. S. Zhou, F. R. Fan, W. Zhang, Z. Y. Zhou, D. Y. Wu, B. Ren, Z. L. Wang and Z. Q. Tian, *Nature*, 2010, **464**, 392–395.
- 90 M. Hu, A. Ghoshal, M. Marquez and P. G. Kik, *J. Phys. Chem. C*, 2010, **114**, 7509–7514.
- 91 S. Mubeen, S. P. Zhang, N. Kim, S. Lee, S. Kramer, H. X. Xu and M. Moskovits, *Nano Lett.*, 2012, **12**, 2088–2094.
- 92 D. Y. Lei, A. I. Fernández-Domínguez, Y. Sonnefraud, K. Appavoo, R. F. Haglund, J. B. Pendry and S. A. Maier, *ACS Nano*, 2012, **6**, 1380–1386.
- 93 C. Ciraci, R. T. Hill, J. J. Mock, Y. Urzhumov, A. I. Fernández-Domínguez, S. A. Maier, J. B. Pendry, A. Chilkoti and D. R. Smith, *Science*, 2012, **337**, 1072–1074.
- 94 H. X. Xu, J. Aizpurua, M. Käll and P. Apell, *Phys. Rev. E: Stat. Phys., Plasmas, Fluids, Relat. Interdiscip. Top.*, 2000, **62**, 4318–4324.
- 95 M. Moskovits, *J. Chem. Phys.*, 1982, **77**, 4408–4416.
- 96 L. V. Brown, H. Sobhani, J. B. Lassiter, P. Nordlander and N. J. Halas, *ACS Nano*, 2010, **4**, 819–832.
- 97 B. Luk'yanchuk, N. I. Zheludev, S. A. Maier, N. J. Halas, P. Nordlander, H. Giessen and C. T. Chong, *Nat. Mater.*, 2010, **9**, 707–715.
- 98 J. Zuloaga, E. Prodan and P. Nordlander, *ACS Nano*, 2010, **4**, 5269–5276.
- 99 Z. Jacob and V. M. Shalaev, *Science*, 2011, **334**, 463–464.
- 100 K. J. Savage, M. M. Hawkeye, R. Esteban, A. G. Borisov, J. Aizpurua and J. J. Baumberg, *Nature*, 2012, **491**, 574–577.